Journal of Thermal Analysis and Calorimetry (2023) 148:7579–7590
https://doi.org/10.1007/s10973-023-12266-2

High thermal conductivity of green nanofluid containing Ag nanoparticles prepared by using solution plasma process with *Paramignya trimera* extract

Nguyen Van Hao[1] · Do Hoang Tung[2] · Truong Thi Thao[1] · Vu Xuan Hoa[1] · Nguyen Hoang Thoan[3] · Pham The Tan[4] · Phan Ngoc Minh[5,6] · Jacek Fal[7] · Gaweł Żyła[7] · Pham Van Trinh[5,6]

Received: 18 July 2022 / Accepted: 8 May 2023 / Published online: 30 May 2023

Abstract

Herein, we present for the first time a quick, easy, effective, and green method for preparing green nanofluids containing silver nanoparticles. The solution plasma method with a high-voltage DC power source and extracts from the *Paramignya trimera* was employed to prepare silver nanoparticles. The obtained results showed that silver nanoparticles were spherical, with a small average size of − 8 nm and fairly uniformly dispersed in solution. Surface plasmon resonance spectra show a strong peak at 410 nm for the prepared samples. The Fourier transform infrared spectra revealed the presence of possible functional groups on the surface of silver nanoparticles. Furthermore, the formation mechanism of silver nanoparticles is also proposed. The effect of the preparation times on the thermal conductivity of nanofluid was also investigated. As a result, the nanofluids prepared with longer preparation times had higher thermal conductivity and the highest improvement of 18.3% was obtained for the nanofluid using 4 min preparation compared to the base fluid. The obtained results indicate promise for a simple, fast, and environmentally friendly method for producing nanofluids containing silver nanoparticles with high thermal conductivity for potential applications.

Keywords Green synthesis · Solution plasma process · Paramignya trimera extract · Silver nanoparticles · Nanofluid · Thermal conductivity

✉ Gaweł Żyła
gzyla@prz.edu.pl

✉ Pham Van Trinh
trinhpv@ims.vast.vn

Nguyen Van Hao
haonv@tnus.edu.vn

Do Hoang Tung
dhtung@iop.vast.ac.vn

Truong Thi Thao
thaott@tnus.edu.vn

Vu Xuan Hoa
hoavx@tnus.edu.vn

Nguyen Hoang Thoan
thoan.nguyenhoang@hust.edu.vn

Pham The Tan
phamthetansp@gmail.com

Phan Ngoc Minh
minhpv@vast.ac.vn; pnminh@vast.ac.vn

Jacek Fal
jacekfal@prz.edu.pl

[1] Institute of Science and Technology, TNU - University of Sciences, Tan Thinh ward, Thái Nguyên, Viet Nam

[2] Institute of Physics, Vietnam Academy of Science and Technology, 18 Hoang Quoc Viet Str., Cau Giay Distr., Hanoi, Vietnam

[3] School of Engineering Physics, Hanoi University of Science and Technology, 1 Dai Co Viet road, Hanoi, Viet Nam

[4] Hung Yen University of Technology and Education, Khoai Chau Distr., Hung Yen, Vietnam

[5] Institute of Materials Science, Vietnam Academy of Science and Technology, 18 Hoang Quoc Viet Str., Cau Giay Distr., Hanoi, Viet Nam

[6] Graduate University of Science and Technology, Vietnam Academy of Science and Technology, 18 Hoang Quoc Viet Str., Cau Giay Distr., Hanoi, Vietnam

[7] Department of Physics and Medical Engineering, Rzeszów University of Technology, 35-959 Rzeszów, Poland

List of symbols

A, *B*, *C*	eq. (7) numerical factors
a	Numerical factor [s^{-1}]
e	Elementary charge
K	Thermal conductivity [W m^{-1} K^{-1}]
T	Temperature [K]
t	Time [s]

Subscripts

aq	Hydrated
bf	Base fluid
nf	Nanofluid

Abbreviations

AgNPs	Silver nanoparticles
EG	Ethylene glycol
FTIR	Fourier transform infrared absorption
GNPs	Graphene nanoplatelets
NFs	Nanofluids
OES	Optical emission spectroscopy

Introduction

Common liquids like water, ethylene glycol (EG), oil, etc., are frequently utilized as heat transfer fluids. However, their inferior thermal performance, they have not demonstrated significant capability for the devices operating at high power. Numerous efforts have been proposed and made to increase the performance of traditional fluids for heat transfer applications. It was presented that the thermophysical properties of such fluids could be easily changed with the addition of nanoparticles [1-4]. The performance of the thermal transfer could be improved with such materials [5-7]. A new class of fluids known as nanofluids (NFs) containing nano-sized particles like Ag, Cu, Ni Al_2O_3, Fe_3O_4, CuO, TiO_2, graphene, and carbon nanotubes showed even better heat transfer performance [5]. The utilization of nanofluids results in an increase in the efficiency of thermal systems evident in a variety of industrial applications [8, 9]. Besides, the necessity of generating ecologically friendly nanofluids has grown in significance [10, 11]. Green technologies involve procedures that do not pose a threat to the environment, the preservation of natural resources, and the introduction of sustainable practices that limit the negative effects of human activity [11]. Recently, some kinds of green nanofluids have been developed and presented (Table 1). In these reports, some nanomaterials such as graphene nanoplatelets (GNPs), carbon nanotubes, metals (Ag), and metal oxides (Al_2O_3, CuO, SiO_2, etc.) used as nanoadditives and the natural extracts from *Gallic Acid, Bio Glycol, Callistemon Viminalis, Neem leaf*, etc., have been used as the reduction or functionalization agents instead of the chemical products [12-20]. Most reports emphasized the need for the development of green nanofluids using simple, cost-effective, safe,

Table 1 Reports on the thermal conductivity of some green nanofluids

References	Nanoadditives	Natural extract	Thermal conductivity Enhancement
[12]	GNPs	Gallic Acid	17.76%
[13]	Al_2O_3–SiO_2	Bio Glycol	30:70 (Al_2O_3:SiO_2) at 70 °C which was at 21.2%
[14]	CuO nanoparticles	Callistemon Viminalis	34% at 9 vol%
[15]	TiO_2–SiO_2	Bioglycol	12.52%
[16]	MWCNTs	Gallic acids	21.510% for a mass fraction of 0.1% at 45 °C
[17]	AgNPs	Neem leaf extracts	32% in heat transfer coefficient
[18]	ZnO	Glycerol	0.7%
[19]	SiO_2 nanoparticles	Rice Bran	38% at 3 vol%
[20]	SiO_2 nanoparticles TiO_2 nanoparticles	Olive Leaf Extract (OLE) Burley Husk (BH)	Higher for $BHSiO_2$ than for OLE-TiO_2 nanoparticles
[21]	GNPs	Clove buds	23%
[22]	GNPs	Gallic Acid	24.18%
[23]	MWCNTs	Clove	20%
[24]	Al_2O_3 particles	Bioglycol	17% and 5% for 1 vol% at 30 and 80 °C
[25]	Carbon/graphene	EFB Pulp	10.16%
[15]	TiO_2–SiO_2 nanoparticles	Bioglycol	12.52% at 3.0 vol% and 0.71% at 0.5 vol %
This work	AgNPs	Paramignya trimera	18.3%

clean, and environmentally friendly synthesis procedures in order to have minimally detrimental effects on public health and the environment [10, 11].

Among nanoadditives, noble metal nanoparticles, such as silver nanoparticles (AgNPs) in particular, are known for their unique thermal-electrical properties [26]. In recent years, AgNPs have attracted much attention from researchers and analysts for applications in many fields, including catalysis, optoelectronics, biomedicine, biosensors, and nanofluids [27, 28]. Using AgNPs as a nanoadditives for nanofluids could improve the thermal conductivity [29]. However, the preparation cost of AgNPs is currently a big barrier to use in commercial nanofluids. Many AgNPs synthesis methods have been proposed, such as chemical reduction and biosynthesis, and laser etching [30, 31]. Each method has its advantages and disadvantages in terms of cost, yield, synthesis time, stability, and dispersion in solution, as well as application purposes [32]. The chemical reduction method can give a high yield and is also the most popular method for the synthesis of silver nanoparticles, due to the use of simple and inexpensive equipment. However, the high cost of toxic, non-environmentally friendly reagents as well as the control of shape, size distribution, monodisperses, and purity of the preparation materials need to be carefully considered. The biosynthesis method is an environmentally friendly and low-cost method, but the synthesis time is long and the size is difficult to control [32]. The laser ablating method has a relatively fast and clean preparation time; however, the high cost due to the need to use expensive pulsed lasers, consuming a large amount of energy, and being quite cumbersome reduces the attractiveness of the method [32]. Several other techniques such as electrochemistry, microplasma, and plasma in a liquid have also been included as a simple and effective solution for the synthesis of large numbers of silver nanoparticles [33]. However, for the electrochemical method, some disadvantages still need to use of more chemicals as an electrolyte, leading to the product purity not being high, increasing cost as well as requiring a long time to manufacture [33], or the microplasma method has the disadvantage that the plasma beam is small, so the production rate of AgNPs is limited [33], while the direct plasma method in the liquid requires a high voltage pulsed power supply which leads to high input costs [34]. The solution-directed plasma method has been widely used to prepare metal nanomaterials, but the mechanism of particle formation remains unclear [34]. Besides, the use of the solution plasma is a promising technique for preparing green nanofluids.

Thus, the goal of this work is to develop for the first time a simple, fast, environmentally friendly, low-cost method to prepare green nanofluids containing AgNPs at room temperature with extracts from *P. trimera* by using the solution plasma technique. This method allows to obtain high thermal conductivity and good stability nanofluid containing AgNPs with small size, well dispersion in solution in a single process for different applications in the electricity and electronics fields.

Experimental

Materials and methods

Paramignya trimera is a tree that was found in the forest on Phu Quoc Island, Vietnam. It was washed several times with tap water and distilled water, then dried at 60 ^{o}C for 12 h. After that, *P. trimera* was cut into small pieces of 1–3 mm, then crushed and dried at 60 ^{o}C for 6 h. Follow-up, 10 g of *P. trimera* powder was mixed with 150 mL distilled water, then boiled at 90 ^{o}C for 120 min under magnetic stirring at 800 rpm. The obtained solution was cooled and filtered twice with Whatman filter paper #1 to get rid of the residue to obtain *P. trimera* extract. The obtained extract was stored at 4^{o}C for gradual use in the preparation of AgNPs.

Preparation of nanofluid containing AgNPs by solution plasma process with *P. trimera* extract

The nanofluids containing AgNPs were prepared by arc discharge solution plasma process as shown in Fig. 1. The reaction vessel includes two electrodes made by a silver rod (99.99% purity, 1 mm in diameter) bent into an L-shape and a platinum rod (2 mm in diameter). The gap between the two electrodes was fixed at 0.2 mm. A mixture of 2 mL of *P. trimera* extract and 30 mL of distilled water was used as the discharge solution. The two electrodes were connected to a high-voltage DC power supply with a potential of 3.0 kV and a current of 0.27 A. The reaction vessel containing the solution and the plasma electrode system was placed in an ultrasonic bath. The discharge time was varied in the range of 30–240 s to prepare the nanofluids. During the preparation process, the color of the solution changed from light yellow to brown depending on the discharge times, indicating the formation of AgNPs in the nanofluid (Fig. 2).

Characterization

The surface plasmon absorption characteristics of AgNPs were measured using a UV–Vis spectrometer (Jassco-V770, Japan) in the spectral range from 200 to 800 nm at a resolution of 0.5 nm. The crystal structure of the samples was measured by a Rigaku D2 X-ray diffraction instrument using a Cu-layer K α radiation source at a wavelength of 1.5418 Å, in the range 10 – 80^{o}. The size, morphological, and composition of AgNPs were observed by TEM images (JEM1010-Jeol) operating at 80 kV. The chemical

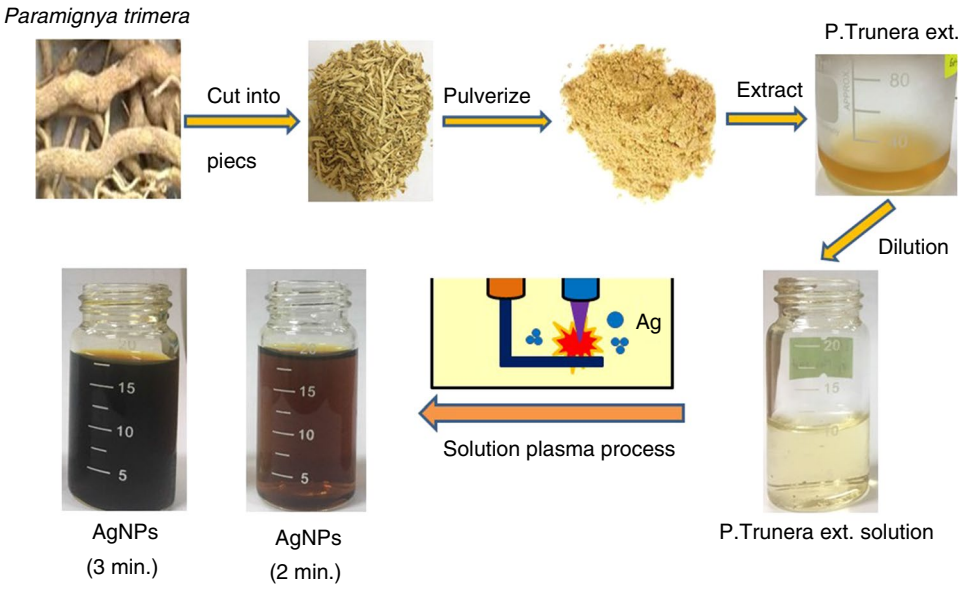

Fig. 1 Schematic view of the preparation process of Ag nanoparticles by solution plasma process with *P. trimera* extraction

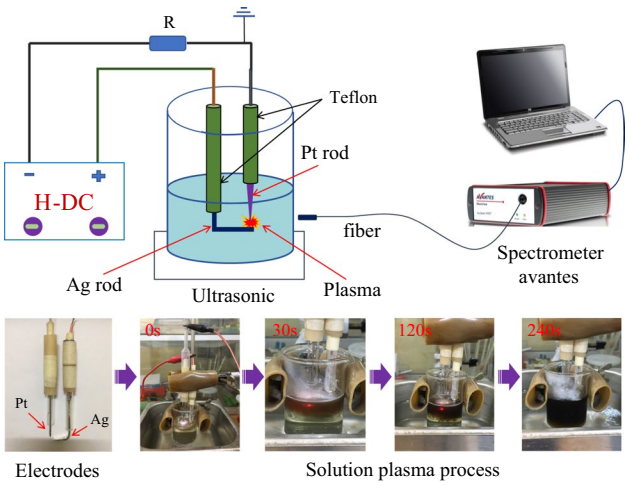

Fig. 2 Schematic diagram of the setup for the AgNPs preparation and OES measurement setup

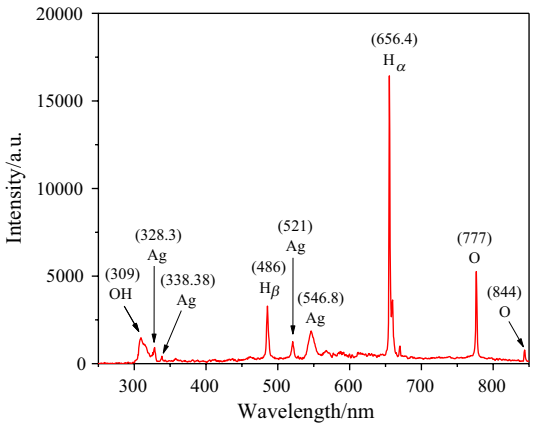

Fig. 3 Optical emission spectra (OES) measured during solution plasma with *P. trimera* extract

bonding characteristics were determined through Fourier transform infrared absorption (FTIR) spectroscopy with a resolution of 4 cm^{-1}(Spectrum Two, PerkinElmer, USA) in the spectral range from 450 to 4000 cm^{-1}. Raman spectra of samples were measured using a Horiba Xplora ONE Raman spectrometer with laser excitation at 532 nm at 10 mW laser power. Optical emission spectroscopy (OES) of the plasma was obtained using a fiber optic spectrometer (AvaSpec-ULS2048, Avantes) with a wavelength range of 200–900 nm and a resolution of 0.5 nm. The HTL-04 an uncertainty of 2.0% provided by Eternal Engineering Equipment Ltd., India, was used to measure the thermal conductivity of the nanofluids in the range of 30–50 ºC.

Results and discussion

Optical emission spectral character

Figure 3 shows the optical emission spectra measured during the solution plasma process in the synthesis of AgNPs with the extract of *P. trimera*. As can be seen, the emission lines were located at 309 nm assigned to OH radical, at 777 nm and 844 nm for O atoms, and at 486 nm and 656.4 nm for H_β and H_α atoms, coexisted in the arc discharge solution [35]. These emission lines are all the result of the dissociation of H_2O [36]. Emissions due to the excited states of Ag atoms are also observed at the 328.3 nm, 338.38 nm, 521 nm, and 546.8 nm. However, the intensities of the emission lines are low, indicating that Ag particles are formed during arc discharge, where

these lines are related to the transitions of Ag neutral [36]. Ag atoms are separated from the Ag electrode when bombarded by plasma species such as H, OH radicals, and O atoms.

Effect of discharge time on the formation of AgNPs

The brown colloidal mixture formed from the solution plasma process containing the extract of *P. trimera* is the visual and clear evidence of the formation of AgNPs (Fig. 2). The brown color of the mixture after solution plasma processing can be attributed to the surface plasmon resonance of the electrons on the surface of AgNPs [37]. The initial color of the solution changed from brown to dark brown and as the arc discharge time increased. The color change of the solution indicated the formation of Ag crystals from the Ag rod. Due to the Ag crystal formation, a sharp and narrow surface plasmon peak was observed at 410 nm (Fig. 4). This can be attributed to the formation of isotropic spherical AgNPs. The biomolecules from the *P. trimera* extract acted not only as a reducing agent of Ag^+ ions to Ag crystals but also as a surfactant to enclose the AgNPs.

The dependence of discharge time on the prepared nanofluid containing AgNPs was investigated. Figure 4a. shows the UV–Vis absorption spectra of the nanofluid containing AgNPs synthesized by the solution plasma method in the presence of *P. trimera* extract using a high-voltage DC source with different discharge times. An increase in absorbance was observed with arc discharge time from 30 to 240 s indicating the enhancement of the formation of AgNPs. The spectrum has only a single peak appearing at about 410 nm. This implied that the AgNPs shape is symmetric. To evaluate the stability of the prepared AgNPs, the UV–Vis absorption spectra of the same sample were measured at three different times (Fig. 4b). The obtained results showed that the absorption spectrum showed no increase in baseline after 4 and 8 months. This demonstrated that no precipitation occurred. However, the slight increase in spectral intensity and slight red-shift in the peak may be due to the reduction in Ag^+ ions produced during plasma discharge in the solution after 4 and 8 months and the growth of Ag ions in the solution of nucleated AgNPs [37]. The obtained results confirm that nanofluid containing AgNPs have good stability and are less prone to agglomeration or the tendency to form large particles. Therefore, it can be concluded that the extract of *P. trimera* is not only a biological reducing agent but also a good surfactant for the nanoparticles dispersed in the solution.

Analysis of physicochemical properties

FTIR spectroscopy was performed to identify the biomolecules and the related functional groups that could be responsible as effective reducing and stabilizing agents of AgNPs during the solution plasma process. Figure 5a presents the FTIR spectrum of the *P. trimera* extract and AgNPs particles. As can be seen, the absorption bands at 3253, 1637, 1050, and 670 cm^{-1} for the *P. trimera* extract and 3367, 1641, 1046, and 654 cm^{-1} for the synthesized AgNPs. The high intensity peaks at 3253 and 3367 cm^{-1} are assigned to the -OH stretching that is possibly caused by phenolic compounds present in the *P. trimera* extract. The peak appearing at 1637 cm^{-1} for *P. trimera* and 1641 cm^{-1} for AgNPs is attributed to the involvement of amide-I binding (–C=O) of the protein as a capturer and stabilizer of AgNPs [38]. The absorption peaks at 1050 cm^{-1} and 1046 cm^{-1} are assigned to the C=O elongation of the alcohol groups [39]. The peaks at 654 and 670 cm^{-1} may be related to the alkyl halides band [40]. In addition, the presence of the peaks located at the spectral range from 621 to 672 cm^{-1} indicates the bending region of the aliphatic chain [41].

To investigate in more detail the possible functional groups of the biopolymer in encapsulating and stabilizing AgNPs, Raman spectroscopy of AgNPs was conducted. The obtained results showed that Raman spectroscopy of AgNPs has spectral peaks at 241, 1346.4, and 1565 cm^{-1} (Fig. 5b). These peaks indicate the interaction between the extract and Ag^+ ions during solution plasma to form AgNPs [42]. The two wide bands at 1346.4 and 1565 cm^{-1} correspond to the

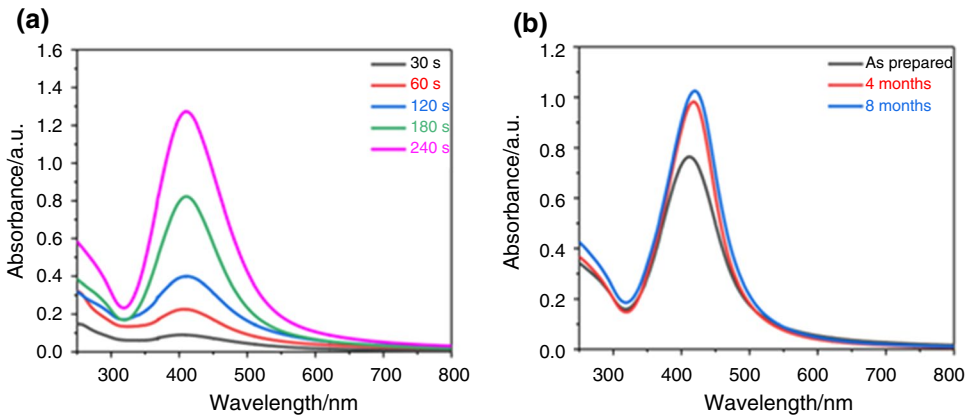

Fig. 4 UV–Vis absorbance spectra of **a** AgNPs prepared by solution plasma process using *P. trimera* extract at different arc discharge times and **b** nanofluid containing AgNPs after 4 and 8 months

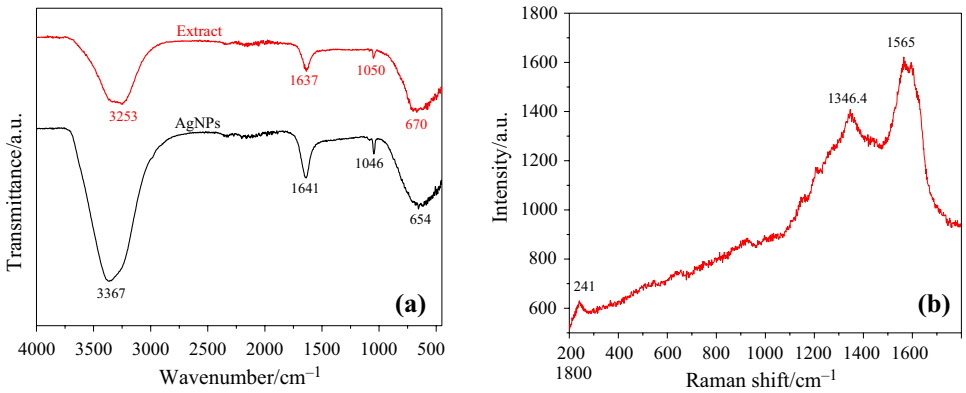

Fig. 5 **a** FTIR spectra of solution containing *P. trimera* extract and AgNPs after solution plasma process with *P. trimera*; **b** Raman spectrum of AgNPs

symmetric and asymmetric C=O stretching oscillations of the carboxylate group, respectively [43]. The spectral peak at 241 cm^{-1} is thought to be the stretching vibration of Ag–N and Ag–O [44]. This peak indicates the formation of a chemical bond between silver and the amino nitrogen, carboxylate groups [44]. It was also confirmed that the *P. trimera* extract encapsulates AgNPs as a surfactant [45].

Analysis of structural and morphological properties

Figure 6a shows the TEM image and particle size distribution of the prepared AgNPs. As can be seen, the prepared AgNPs have a spherical shape with an average size of 8 nm. The fact that the AgNPs are distributed fairly uniformly throughout the solution. This proved that the *P. trimera* extract solution can effectively encapsulate the AgNPs surface. Recently, the biosynthesis of AgNP by using plant extracts as reducing agents has been reported [46-52]. Escarcega-Gonzalez et.al. reposted that AgNPs with spherical shapes with the size from 10 to 22 nm were synthesized by using *Acacia rigidula* extract as a reducing and capping agent. Baghizadeh and coworkers prepared AgNPs with an average diameter of 7.5 nm using the extract of *Calendula Officinalis* seed [46]. Similarly, Pragathiswaran et.al. also used a plant extract from *Cissus quadrangularis* leaf to prepare spherical AgNPs [47]. Almalah et.al. reported that the extract of *Cinnamomum zylinicum* could be used to prepare spherical AgNPs with a diameter in the range of 10-79 nm [49]. Other reports from Dhar and coworkers also presented the results on the synthesis of AgNPs with the size of 16–29 nm using the extract of *Phyllanthus emblica* fruit [50]. According to the above comments, the obtained results are more effective than preparing smaller AgNPs particles with a range size from 2 to 16 nm when using *P. trimera* extract as a reducing agent.

X-ray diffraction (XRD) pattern of AgNPs prepared by solution plasma process with the extract of *P. trimera* is shown in Fig. 7. The obtained results indicated that the face-centered cubic crystal structure of AgNPs has characteristic diffraction peaks at 37.5; 43.7; 63.92, and 76.94^o corresponding to the (111), (200), (220), and (311) planes, respectively. The diffraction peak at 37.5 ^{o} has a strong diffraction intensity indicating the preferred direction of the silver crystal along the (111) plane. This result is consistent with the results of previous studies by other authors [53, 54]. The diffraction phase of the prepared AgNPs sample shows that the crystal lattice of AgNPs synthesized by the solution plasma process with the extract of *P. trimera* is not affected by other molecules.

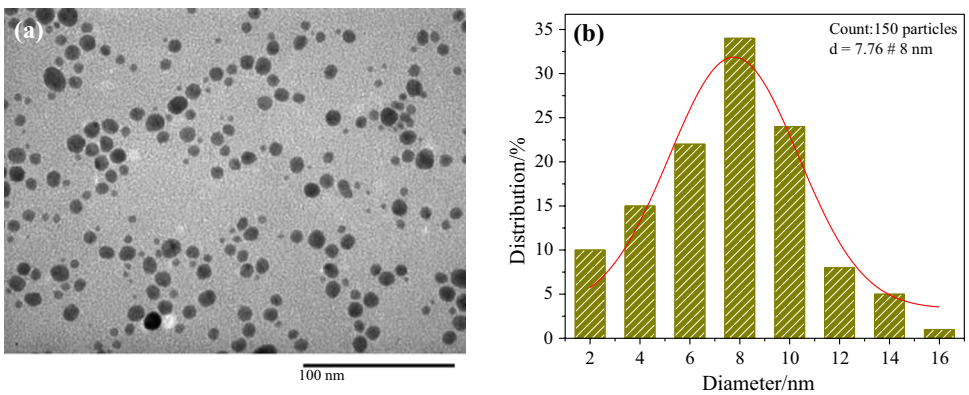

Fig. 6 **a** TEM image and **b** the size distribution of the AgNPs

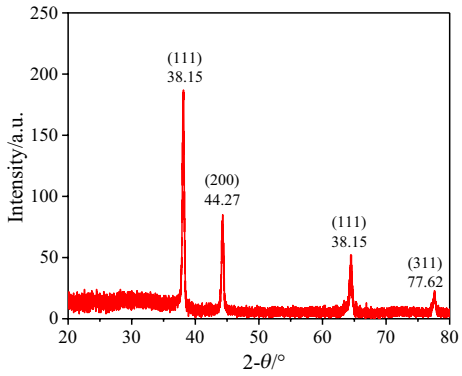

Fig. 7 XRD pattern of AgNPs prepared by the solution plasma process using the extract of *P. trimera* as a reducing agent

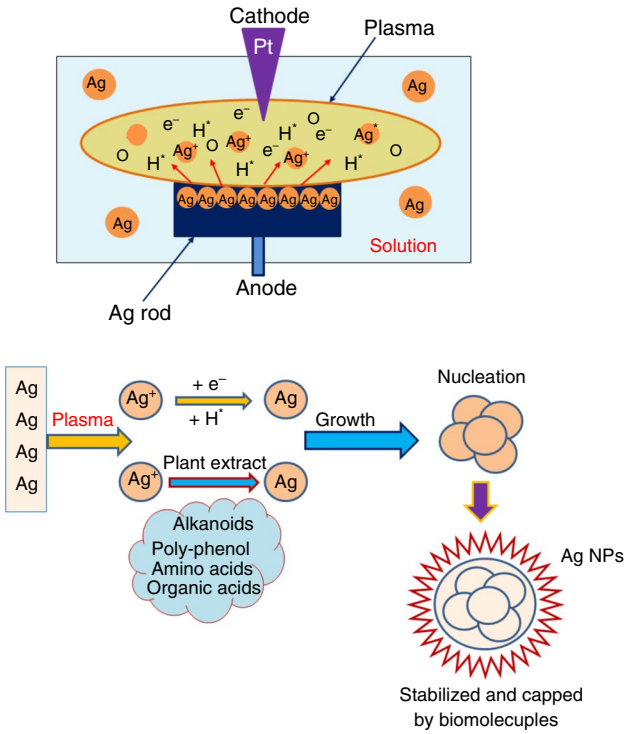

Fig. 8 Scheme illustrating the supposed mechanism of formation of Ag nanoparticles during a solution plasma arc discharge and biosynthesis

Proposed AgNPs formation mechanism

Figure 8 illustrates the possible formation mechanism of AgNPs during the solution plasma process. The formation of AgNPs could be affected by the strong electric field, sputtering, and arc discharge effects that occurred in the solution plasma. The details of this formation are explained below:

$$Ag \rightarrow Ag^{+}(after\ arc\ plasma) \quad (1)$$

$$Ag^{+} + H^{*} \rightarrow Ag + H^{+} \quad (2)$$

$$Ag^{+} + e^{-} \rightarrow Ag \quad (3)$$

$$biomolecules + Ag^{+} + e^{-}_{aq} \rightarrow Ag \quad (4)$$

At the Ag anode, Ag is evaporated as Ag^{+} ions by arc discharge (Eq. (1)). In addition, during the discharge in liquids, the species such as ions, electrons, and neutral molecules can be generated, and their density is proportional to the discharge time. The evaporation of metal ionization mainly depends on the applied voltage, the current, and the distance between electrodes and metal surface area [55]. After the generation of Ag ions in solution, Ag^{+} ions can be rapidly reduced by hydrogen radicals or e^{-} generated in the solution plasma to form AgNPs as shown in Equs. (2) and (3). By the reduction reaction, hydrogen ions are produced, which lowers the pH of the solution (2). The heat generated during the arc discharge and the discharge environment also influences the formation of nanoparticles [55]. Besides, the formation of AgNPs also contributes to the nucleation by hydrated electrons (e_{aq}) which act as a strong reducing agent as shown in Equation (4) [56]. Phenolics are aromatic rings with one or more hydroxyl groups present in the biologically active substance. The antioxidant and redox properties of phenolic compounds help in the absorption and neutralization of free radicals, singlet, and triplet quenching or rapid peroxyte decomposition. It is this resonance in phenol, which rapidly reduces Ag ions to Ag atoms [57]. Formation of AgNPs through nucleation and growth due to attractive van der Waals forces between Ag atoms. The synthetic AgNPs are bound to the hydroxyl group of the biomolecule to prevent their large-scale aggregation [58].

Thermal conductivity of nanofluids

Figure 9a and Table 2 show the thermal conductivity (K_{nf}) of nanofluids containing AgNPs prepared at different times versus measured temperatures. As a result, the K_{nf} of nanofluids enhanced with the increase in time. At 30^{o}C, the thermal conductivity of nanofluids with 240 s plasma discharge was determined to be 0.682 $W.m^{-1}K^{-1}$, which is higher than 12.3% compared to the base liquid (0 s). At 55 ^{o}C, the experimental results indicated that the maximum enhancement of 18.3% is observed for the nanofluids prepared in 240 s compared with the base fluid, and this behavior is valid for all tested temperatures. The obtained value is in line with the other reports on other green nanofluids listed in Table 1. Some reports presented better thermal conductivity enhancements when using advanced nanoadditives (GNPs CNTs) and/or high concentrations [15-25]. Sone et.al., reported on the preparation of nanofluid containing p-type

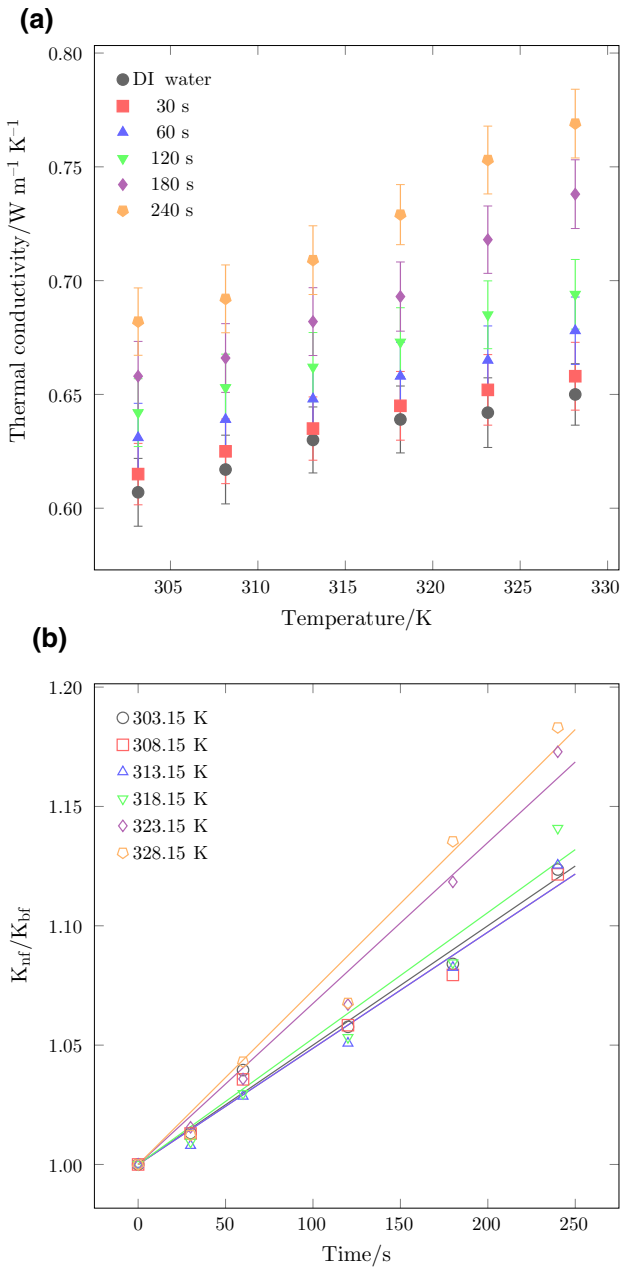

Fig. 9 **a** Thermal conductivity of nanofluids versus synthesis time and measured temperatures and **b** The thermal conductivity ratio of the nanofluids prepared at different times for various temperatures

CuO nanoparticles biosynthesized using *Callistemon viminalis* flower extract as a chelating agent [14]. The enhancement of the thermal conductivity reached up to 34% with 9 vol.% CuO [14]. Akram et. al., also prepared green nanofluids containing hydrophilic functionalized CNTs with 21.5% enhancement in thermal conductivity when using the free radical grafting of Gallic Acids [16]. High thermal conductivity of green nanofluids containing SiO_2 nanoparticles with 38% enhancement for 3 vol.% was reported by Ranjbarzadeh and coworkers [19]. Sadri et.al., reported a 24% enhancement in the thermal conductivity for the green nanofluid containing GNPs and using Gallic Acid for the surface functionalization of GNPs [22]. Compared to these reports, this study showed promise in terms of fast and easy for mass production of high-performance green nanofluids.

To evaluate the performance of the prepared nanofluid, the following linear function could be used to express the relationship between the K of the nanofluids and the preparation times:

$$\frac{K_{nf}}{K_{bf}} = 1 + a \cdot t, \tag{5}$$

where K_{nf} and K_{bf} are the thermal conductivity of nanofluid, base fluid, respectively, which depended on the prepared times, while a is a numerical factor related to temperature.

To find the best value of a factor, Origin Pro 9.1 was employed and the results were presented in Table 3 where R^2 was better than 0.9999.

Besides, the K_{nf} of the prepared nanofluids was increased when measured at higher temperatures. The increase in thermal conductivity is close to linear with prepared time (Figure 9b). However, changes in thermal conductivity with temperature are nonlinear and can be described by following function:

$$a = A + B \cdot T + C \cdot T^2, \tag{6}$$

where A, B, and C are numerical factors. The dependence of a as function of temperature and corresponding fitting function (6) was presented in Fig. 10.

By substituting Equations (6) to (5), universal function of thermal conductivity ratio for temperature and synthesis time in measured ranges can be obtained:

Table 2 Thermal conductivity, K_{nf} [W·m^{-1}·K^{-1}], of nanofluids at various temperatures and synthesis time

Time/s	Temperature/K					
	303.15	308.15	313.15	318.15	323.15	328.15
0	0.607	0.617	0.63	0.639	0.642	0.650
30	0.615	0.625	0.635	0.645	0.652	0.658
60	0.631	0.639	0.648	0.658	0.665	0.678
120	0.642	0.653	0.662	0.673	0.685	0.694
180	0.658	0.666	0.682	0.693	0.718	0.738
240	0.682	0.692	0.709	0.729	0.753	0.769

Table 3 Values of fitting parameters for the Equation (5)

Time/s	a × 10^{-4}	R^2
0	5.001	0.99997
30	4.867	0.99998
60	4.867	0.99996
120	5.277	0.99992
180	6.745	0.99994
240	7.290	0.99990

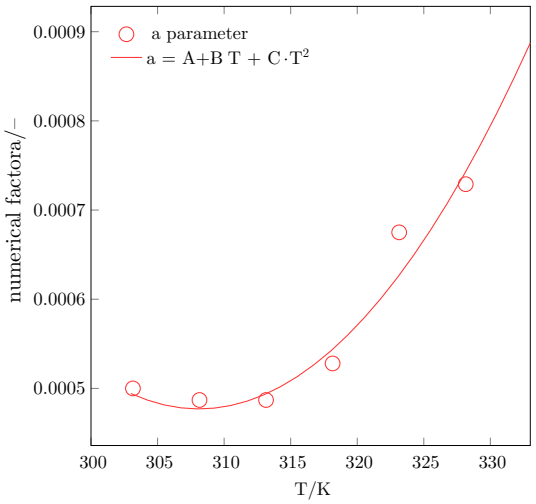

Fig. 10 Values of fitting parameter *a*

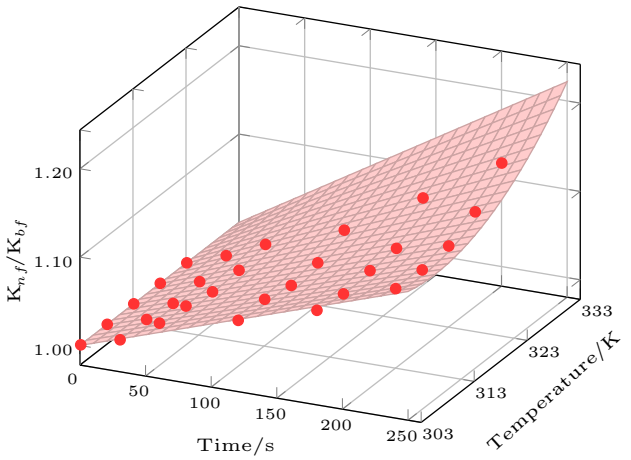

Fig. 11 Thermal conductivity enhancement of nanofluids versus synthesis time and temperature. Points are experimental data, and surface is obtained by fitting of function (7)

$$\frac{K_{\mathrm{nf}}}{K_{\mathrm{bf}}} = 1 + A \cdot t + B \cdot t \cdot T + C \cdot t \cdot T^2. \tag{7}$$

The values of fitted parameters for Equation (7) were obtained using OriginPro 9.1 with R^2 coefficient better than 0.976 and were equal to 0.06332, -4.07936×10^{-4}, and 6.62013×10^{-7} for *A*, *B*, and *C*, respectively. The graphical form of this fitting is presented in Fig. 10 where the good agreement of experimental data with the proposed universal function (7) was also confirmed.

The enhancement of the *K* of the nanofluid prepared in longer time could be due to the increase in AgNPs concentration. According to Baby et al., the characteristics of the nanoparticle and the base fluid have a significant impact on the linearity/nonlinearity of thermal conductivity [59]. The percolation effect causes the mean free route of nanoparticles to shorten or the volume fraction to rise, increasing the frequency of lattice vibration and improving the thermal conductivity of the nanofluid [59]. Li and coworkers claim that the increase in thermal conductivity with temperature might be explained [60]. According to Li et al., Brownian motion and the agglomeration and viscosity changes of nano additives with temperature are significant elements in explaining the temperature dependency of the thermal conductivity of nanofluids [60]. Li predicted that an increase in temperature would have the following effects: (i) a decrease in the agglomeration of nanoadditives in the nanofluid due to a decrease in the surface energy of the nanoadditives and (ii) an improvement in the Brownian motion due to a decrease in viscosity [60]. The Brownian motion is a well-known important mechanism for improving the thermal conductivity of nanofluids [61]. As a result, nanofluids' thermal conductivity rises as temperature rises.

Conclusions

We have prepared high thermal conductivity nanofluids containing AgNPs using a quick, easy, effective, and green method via a solution plasma method using a high voltage DC power source and extracts from the *P. trimera* with some conclusions as follows:

a. The prepared AgNPs were spherical, with a small average size of 8 nm with the surface plasmon resonance spectra show a strong peak at 410 nm. FTIR and Raman analysis demonstrated the formation of a chemical bond between silver and the amino nitrogen, carboxylate groups and the *P. trimera* extract encapsulates AgNPs as a surfactant leading to remain the stability of green nanofluids.
b. The formation mechanism of AgNPs is also proposed in which the attractive van der Waals forces that exist between individual Ag atoms contribute to the nucleation and growth processes. The presence of the hydroxyl

group of the biomolecule on the surface prevents the aggregation of AgNPs.

c. Increasing the preparation times for nanofluids resulted in an improvement in thermal conductivity, and the green nanofluid prepared with 240 s showed the highest improvement of 18.3% compared to base fluid (0 s).

d. The obtained results demonstrated the promise of the proposed method to prepare the high thermal conductivity and good stability nanofluid containing AgNPs with small size, well dispersion in solution in a single process for potential applications such as heat dissipation for the electricity and electronic devices, solar energy collectors, antibacterial.

Acknowledgements This research was supported by Project of the TNU-University of Sciences in Vietnam under Grand number CS2021-TN06-15. GŻ. wish to thank Jolanta Sobczak (Rzeszow University of Technology) for technical support.

Author contributions Conceptualization was contributed by N.V.H. G.Ż. and P.V.T.; methodology was contributed by N.V.H., P.V.T., and D.H.T.; validation was contributed by P.T.T., T.T.T., and D.H.T.; formal analysis was contributed by N.V.H., P.T.T., and N.H.T., J.F.; investigation was contributed by T.T.T.., V.X.H., and N.V.H.; writing—original draft preparation, was contributed by N.V.H., J.F., G.Ż., and P.V.T.; writing—review and editing, was contributed by N.V.H., G.Ż., and P.V.T.; supervision was contributed by P.N.M. All authors have read and agreed to the published version of the manuscript.

Declarations

Conflict of interest The authors declare that they have no conflict of interest.

References

1. Qiu L, Zhu N, Feng Y, Michaelides EE, Żyła G, Jing D, Zhang X, Norris PM, Markides CN, Mahian O. A review of recent advances in thermophysical properties at the nanoscale: from solid state to colloids. Phys Rep. 2020;843:1–81.
2. Hamzat AK, Omisanya MI, Sahin AZ, Oyetunji OR, Olaitan NA. Application of nanofluid in solar energy harvesting devices: a comprehensive review. Energy Convers Manage. 2022;266: 115790.
3. Mehta B, Subhedar D, Panchal H, Said Z. Synthesis, stability, thermophysical properties and heat transfer applications of nanofluid-a review. J Molecul Liq. 2022;6(5): 120034.
4. Patel J, Soni A, Barai DP, Bhanvase BA. "A minireview on nanofluids for automotive applications: Current status and future perspectives." Appl Ther Eng , 2022; p. 119428
5. Modi K, Patel P, Patel S. Applicability of mono-nanofluid and hybrid-nanofluid as a technique to improve the performance of solar still: a critical review. J Clean Product. 2023;3: 135875.
6. Alshuhail LA, Shaik F, Sundar LS. Thermal efficiency enhancement of mono and hybrid nanofluids in solar thermal applications-a review. Alex Eng J. 2023;68:365–404.
7. Pérez Vallejo J, Iglesias Prado JI, Lugo Latas L. *et al.*, "Hybrid or mono nanofluids for convective heat transfer applications. A critical review of experimental research." Appl Ther Eng 2022; 203: 117926
8. Maghrabie HM, Olabi A, Sayed ET, Wilberforce T, Elsaid K, Doranehgard MH, Abdelkareem MA. "Microchannel heat sinks with nanofluids for cooling of electronic components: Performance enhancement, challenges, and limitations," Ther Sci Eng Progress 2022; p. 101608
9. Wang Q, Yang L, Zhao N, Xu G, Song J, Jin X, Li X, Liu S. "A review of applications of plasmonic and conventional nanofluids in solar heat collection," Appl Ther Eng, 2022; p. 119476
10. Pereira JE, Moita AS, Moreira AL."The pressing need for green nanofluids: a review." J Environ Chem Eng 2022; p 107940.
11. Kumar LH, Kazi S, Masjuki H, Zubir M. A review of recent advances in green nanofluids and their application in thermal systems. Chem Eng J. 2022;429: 132321.
12. Kumar LH, Kazi S, Masjuki H, Zubir M, Jahan A, Bhinitha C. Energy, exergy and economic analysis of liquid flat-plate solar collector using green covalent functionalized graphene nanoplatelets. Appl Therm Eng. 2021;192: 116916.
13. Johari MNI, Zakaria IA, Azmi W, Mohamed W. Green bio glycol $Al_2O_3 - SiO_2$ hybrid nanofluids for pemfc: the thermal-electrical-hydraulic perspectives. Int Commun Heat Mass Transfer. 2022;131: 105870.
14. Sone B, Diallo A, Fuku X, Gurib-Fakim A, Maaza M. Biosynthesized CuO nano-platelets: physical properties & enhanced thermal conductivity nanofluidics. Arab J Chem. 2020;13(1):160–70.
15. Zainon S, Azmi W. Stability and thermo-physical properties of green bio-glycol based TiO_2-SiO_2 nanofluids. Int Commun Heat Mass Transfer. 2021;126: 105402.
16. Akram N, Hosseini M, Sadri R, Kazi S, Kasaeian A, Yarmand H, Hooman K, Ahmad R. A facile, green fabrication of aqueous nanofluids containing hydrophilic functionalized carbon nanotubes toward improving heat transfer in a closed horizontal flow passage. Powder Technol. 2022;404: 117451.
17. Kulkarni HR, Dhanasekaran C, Rathnakumar P, Sivaganesan S. Experimental study on thermal analysis of helical coil heat exchanger using green synthesis silver nanofluid. Mater Today Proc. 2021;42:1037–42.
18. Sengwa R, Saraswat M, Dhatarwal P. Comprehensive characterization of glycerol/ZnO green nanofluids for advances in multifunctional soft material technologies. J Mol Liq. 2022;355: 118925.
19. Ranjbarzadeh R, Moradikazerouni A, Bakhtiari R, Asadi A, Afrand M. An experimental study on stability and thermal conductivity of water/silica nanofluid: eco-friendly production of nanoparticles. J Clean Prod. 2019;206:1089–100.
20. Okonkwo EC, Essien EA, Abid M, Kavaz D, Ratlamwala TA. Thermal performance analysis of a parabolic trough collector using water-based green-synthesized nanofluids. Sol Energy. 2018;170:658–70.
21. Sadri R, Hosseini M, Kazi SN, Bagheri S, Abdelrazek AH, Ahmadi G, Zubir N, Ahmad R, Abidin NIZ. A facile, bio-based,

novel approach for synthesis of covalently functionalized graphene nanoplatelet nano-coolants toward improved thermophysical and heat transfer properties. J Colloid Interface Sci. 2018;509:140–52.
22. Sadri R, Hosseini M, Kazi S, Bagheri S, Ahmed S, Ahmadi G, Zubir N, Sayuti M, Dahari M. Study of environmentally friendly and facile functionalization of graphene nanoplatelet and its application in convective heat transfer. Energy Convers Manage. 2017;150:26–36.
23. Sadri R, Hosseini M, Kazi S, Bagheri S, Zubir N, Solangi K, Zaharinie T, Badarudin A. A bio-based, facile approach for the preparation of covalently functionalized carbon nanotubes aqueous suspensions and their potential as heat transfer fluids. J Colloid Interface Sci. 2017;504:115–23.
24. Yarmand H, Gharehkhani S, Shirazi SFS, Amiri A, Montazer E, Arzani HK, Sadri R, Dahari M, Kazi S. Nanofluid based on activated hybrid of biomass carbon/graphene oxide: synthesis, thermo-physical and electrical properties. Int Commun Heat Mass Transf. 2016;72:10–5.
25. Shirazi SFS, Gharehkhani S, Yarmand H, Badarudin A, Metselaar HSC, Kazi SN. Nitrogen doped activated carbon/graphene with high nitrogen level: green synthesis and thermo-electrical properties of its nanofluid. Mater Lett. 2015;152:192–5.
26. Xu L, Wang Y-Y, Huang J, Chen C-Y, Wang Z-X, Xie H. Silver nanoparticles: synthesis, medical applications and biosafety. Theranostics. 2020;10(20):8996.
27. Kang H, Buchman JT, Rodriguez RS, Ring HL, He J, Bantz KC, Haynes CL. Stabilization of silver and gold nanoparticles: preservation and improvement of plasmonic functionalities. Chem Rev. 2018;119(1):664–99.
28. Chen Y, Fan Z, Zhang Z, Niu W, Li C, Yang N, Chen B, Zhang H. Two-dimensional metal nanomaterials: synthesis, properties, and applications. Chem Rev. 2018;118(13):6409–55.
29. Vallejo JP, Sani E, Żyła G, Lugo L. Tailored silver/graphene nanoplatelet hybrid nanofluids for solar applications. J Mol Liq. 2019;296: 112007.
30. Panáček A, Kvitek L, Prucek R, Kolář M, Večeřová R, Pizúrová N, Sharma VK, â. Nevěčná T, Zbořil R. "Silver colloid nanoparticles: synthesis, characterization, and their antibacterial activity." J Phys Chem B, 2006; 110(33),16248–16253
31. Sportelli MC, Izzi M, Volpe A, Clemente M, Picca RA, Ancona A, Lugarà PM, Palazzo G, Cioffi N. The pros and cons of the use of laser ablation synthesis for the production of silver nanoantimicrobials. Antibiotics. 2018;7(3):67.
32. Iravani S, Korbekandi H, Mirmohammadi SV, Zolfaghari B. Synthesis of silver nanoparticles: chemical, physical and biological methods. Res Pharm Sci. 2014;9(6):385.
33. Shuaib U, Hussain T, Ahmad R, Zakaullah M, Mubarik FE, Muntaha ST, Ashraf S. Plasma-liquid synthesis of silver nanoparticles and their antibacterial and antifungal applications. Mater Res Express. 2020;7(3): 035015.
34. Hinokuma S, Shimanoe H, Kawabata Y, Matsuki S, Kiritoshi S, Machida M. Effects of support materials and silver loading on catalytic ammonia combustion properties. Catal Today. 2018;303:2–7.
35. Yoshida T, Yamamoto N, Mizutani T, Yamamoto M, Ogawa S, Yagi S, Nameki H, Yoshida H. Synthesis of ag nanoparticles prepared by a solution plasma method and application as a cocatalyst for photocatalytic reduction of carbon dioxide with water. Catal Today. 2018;303:320–6.
36. Kim H-J, Shin J-G, Park C-S, Kum DS, Shin BJ, Kim JY, Park H-D, Choi M, Tae H-S. In-liquid plasma process for size-and shape-controlled synthesis of silver nanoparticles by controlling gas bubbles in water. Materials. 2018;11(6):891.
37. Shankar SS, Ahmad A, Sastry M. Geranium leaf assisted biosynthesis of silver nanoparticles. Biotechnol Prog. 2003;19(6):1627–31.
38. Masum MMI, Siddiqa MM, Ali KA, Zhang Y, Abdallah Y, Ibrahim E, Qiu W, Yan C, Li B. Biogenic synthesis of silver nanoparticles using phyllanthus emblica fruit extract and its inhibitory action against the pathogen acidovorax oryzae strain rs-2 of rice bacterial brown stripe. Front Microbiol. 2019;10:820.
39. Chinnasamy G, Chandrasekharan S, Bhatnagar S. Biosynthesis of silver nanoparticles from melia azedarach: Enhancement of antibacterial, wound healing, antidiabetic and antioxidant activities. Int J Nanomed. 2019;14:9823.
40. Bagherzade G, Tavakoli MM, Namaei MH. Green synthesis of silver nanoparticles using aqueous extract of saffron (crocus sativus l.) wastages and its antibacterial activity against six bacteria. Asian Pac J Trop Biomed. 2017;7(3):227–33.
41. Hamouda RA, Hussein MH, Abo-Elmagd RA, Bawazir SS. Synthesis and biological characterization of silver nanoparticles derived from the cyanobacterium oscillatoria limnetica. Sci Rep. 2019;9(1):1–17.
42. Ali M, Kim B, Belfield KD, Norman D, Brennan M, Ali GS. Green synthesis and characterization of silver nanoparticles using artemisia absinthium aqueous extract?a comprehensive study. Mater Sci Eng, C. 2016;58:359–65.
43. Mukherjee P, Roy M, Mandal B, Dey G, Mukherjee P, Ghatak J, Tyagi A, Kale S. Green synthesis of highly stabilized nanocrystalline silver particles by a non-pathogenic and agriculturally important fungus t. asperellum. Nanotechnology. 2008;19(7): 075103.
44. Chowdhury J, Ghosh M. Concentration-dependent surface-enhanced raman scattering of 2-benzoylpyridine adsorbed on colloidal silver particles. J Colloid Interface Sci. 2004;277(1):121–7.
45. Kora AJ, Sashidhar R, Arunachalam J. Gum kondagogu (cochlospermum gossypium): a template for the green synthesis and stabilization of silver nanoparticles with antibacterial application. Carbohyd Polym. 2010;82(3):670–9.
46. Escárcega-González CE, Garza-Cervantes JA, Vazquez-Rodríguez A, Montelongo-Peralta LZ, Treviño-Gonzalez MT, Castro EDB, Saucedo-Salazar EM, Morales RC, Soto DR, González FT, et al. In vivo antimicrobial activity of silver nanoparticles produced via a green chemistry synthesis using acacia rigidula as a reducing and capping agent. Int J Nanomed. 2018;13:2349.
47. Baghizadeh A, Ranjbar S, Gupta VK, Asif M, Pourseyedi S, Karimi MJ, Mohammadinejad R. Green synthesis of silver nanoparticles using seed extract of calendula officinalis in liquid phase. J Mol Liq. 2015;207:159–63.
48. Pragathiswaran C, Violetmary J, Faritha A, Selvarani K, Nawas PM. Photocatalytic degradation, sensing of Cd^{2+} using silver nanoparticles synthesised from plant extract of cissus quadrangularis and their microbial activity. Mater Today Proc. 2021;45:3348–56.
49. Almalah HI, Alzahrani HA, Abdelkader HS. Green synthesis of silver nanoparticles using cinnamomum zylinicum and their synergistic effect against multi-drug resistance bacteria. J Nanotechnol Res. 2019;1(3):95–107.
50. Dhar SA, Chowdhury RA, Das S, Nahian MK, Islam D, Gafur MA. Plant-mediated green synthesis and characterization of silver nanoparticles using phyllanthus emblica fruit extract. Mater Today Proc. 2021;42:1867–71.
51. Kambale EK, Nkanga CI, Mutonkole B-PI, Bapolisi AM, Tassa DO, Liesse J-MI, Krause RW, Memvanga PB. Green synthesis of antimicrobial silver nanoparticles using aqueous leaf extracts from three congolese plant species (brillantaisia patula, crossopteryx febrifuga and senna siamea). Heliyon. 2020;6(8): e04493.
52. Adewale OB, Egbeyemi KA, Onwuelu JO, Potts-Johnson SS, Anadozie SO, Fadaka AO, Osukoya OA, Aluko BT, Johnson J, Obafemi TO, et al. Biological synthesis of gold and silver

nanoparticles using leaf extracts of crassocephalum rubens and their comparative in vitro antioxidant activities. Heliyon. 2020;6(11): e05501.
53. Chen S, Kimura K. Synthesis of thiolate-stabilized platinum nanoparticles in protolytic solvents as isolable colloids. J Phys Chem B. 2001;105(23):5397–403.
54. Behravan M, Panahi AH, Naghizadeh A, Ziaee M, Mahdavi R, Mirzapour A. Facile green synthesis of silver nanoparticles using berberis vulgaris leaf and root aqueous extract and its antibacterial activity. Int J Biol Macromol. 2019;124:148–54.
55. Pootawang P, Saito N, Takai O, Lee S-Y. Synthesis and characteristics of Ag/Pt bimetallic nanocomposites by arc-discharge solution plasma processing. Nanotechnology. 2012;23(39): 395602.
56. Nel A, Xia T, Madler L, Li N. "Toxic potential of materials at the nanolevel." science 2006; 311(5761), 622–627
57. Bose D, Chatterjee S. Antibacterial activity of green synthesized silver nanoparticles using vasaka (justicia adhatoda l.) leaf extract. Indian J Microbiol. 2015;55(2):163–7.
58. Mikhailova EO. Silver nanoparticles: mechanism of action and probable bio-application. J Funct Biomater. 2020;11(4):84.
59. Baby TT, Sundara R. Synthesis and transport properties of metal oxide decorated graphene dispersed nanofluids. J Phys Chem C. 2011;115(17):8527–33.
60. Yu-Hua L, Wei Q, Jian-Chao F. Temperature dependence of thermal conductivity of nanofluids. Chin Phys Lett. 2008;25(9):3319.
61. Chon CH, Kihm KD, Lee SP, Choi SU. Empirical correlation finding the role of temperature and particle size for nanofluid (al 2 o 3) thermal conductivity enhancement. Appl Phys Lett. 2005;87(15): 153107.